

BrainTGL:Temporal Graph representation learning for brain network by Exploiting Graph Temporal Information

Tong Zheng, Peng Cao, Tianshun Hong, Guangqi Wen, Huiwen Bao, Xiaoli Liu, Jinzhu Yang, Osmar Zaiane

Abstract—The dynamic functional connectivity analysis provides valuable information for understanding functional brain activity underlying different cognitive processes. Modeling spatio-temporal dynamics in functional brain networks is critical for underlying the functional mechanism of human brain. In our study, we propose an end-to-end framework called temporal graph representation learning for brain network (BrainTGL), which thoroughly captures spatio-temporal features in resting-state functional magnetic resonance imaging (rs-fMRI) data. Specifically, we first transform rs-fMRI time-series into temporal multi-graph using sliding window technique. A temporal multi-graph clustering is then designed to eliminate the inconsistency of the temporal multi-graph series. Then, a dual temporal graph learning LSTM (DTG-LSTM) is further proposed to capture the spatio-temporal embedding for temporal graphs. At last, an ensemble strategy is finally designed to improve the performance with multiple window parameters rather than exploiting an optimal parameter. Extensive experiments on autism brain imaging data exchange (ABIDE) and human connectome project (HCP) datasets show the effectiveness of BrainTGL. BrainTGL achieves state-of-art accuracy on both datasets. Furthermore, the obtained clustering results are consistent with the previous neuroimaging-derived evidence of biomarkers for autism spectrum disorder (ASD).

Index Terms—Dynamic brain network, automated diagnosis, resting-state fMRI, Spatio-temporal modeling

I. INTRODUCTION

The brain is an exceptionally complex system and understanding its functional organization is the goal of modern neuroscience. Over the past decade, understanding the

Manuscript submitted August 9, 2021. This research was supported by the National Natural Science Foundation of China (No.62076059) and the Fundamental Research Funds for the Central Universities (No. N2016001). (Corresponding author: Peng Cao.)

Tong Zheng and Guangqi Wen are with the Computer Science and Engineering, Northeastern University, Shenyang, China.

Peng Cao and Jinzhu Yang are with the Computer Science and Engineering, Northeastern University, Shenyang, China and also with Key Laboratory of Intelligent Computing in Medical Image of Ministry of Education, Northeastern University, Shenyang, China. (e-mail: caopeng@mail.neu.edu.cn).

Huiwen Bao is with the Business Administration, Northeastern University, Shenyang, China.

Xiaoli Liu is with Alibaba A.I. Labs.

Osmar Zaiane is with Amii, University of Alberta, Edmonton, Alberta, Canada.

functional mechanisms of human brain has been one of the most important research directions in clinical neuroscience. In particular, advanced neuroimaging techniques, such as magnetic resonance imaging (MRI) and positron emission tomography (PET), have been developed to explore the functional mechanisms related to a specific neurological disorder or cognitive stimuli [1]. Functional magnetic resonance imaging (fMRI) that measures the changes of blood oxygenation level-dependent (BOLD) signal in a noninvasive manner has become the most common tool to explore functional connectivity (FC) in the brain. It has been widely used in the research of cognitive neuroscience, medical, and clinical applications. Compared with sMRI, since fMRI [2] is able to measure the changes in hemodynamics caused by neuron activity at a series of time points for the whole brain, it has been widely applied in the research of brain dysfunction diseases. The BOLD signal of resting-state fMRI (rs-fMRI) characterizes the intrinsic functional organization of the human brain by measuring its spontaneous activity at rest.

FC is defined as the statistical dependency between different brain regions and has been quantified through the computation of pearson's correlation between regions-of-regions (ROIs) [3], [4]. The previous work has illustrated that the different brain regions still actively interact during rest. Therefore, rs-fMRI has been widely used as one of the major tools to investigate and explore FC [?], [5]–[8]. We particularly focus on modeling the whole brain rs-fMRI as a network, which is called as functional brain networks (FBN), where the observed brain activity is modeled as a network of inter-regional functional associations. Most of the work typically represents the temporal relationships between different brain regions during resting states via pearson's correlation based FC, assuming that FC of the human brain is stationary throughout the whole fMRI recording period [5], [7], [8]. The resulting FBN can be analyzed with various graph learning-based methods. Traditional graph-based analyses for FBN summarize the FC for each node into a single number using graph theoretical metrics. Motivated by the success of deep learning on grid data, efforts have been made to extend CNN (a natural way to represent many forms of data, including fMRI data) to graphs. Kipf & Welling proposed graph convolutional networks (GCN) combining structure information and node features in the learning process as a graph embedding model.

Recent work has applied GCN on the functional network derived from rs-fMRI data to extract latent features from the graph [9], [10] and has recently proven to deliver generalized solutions in disease prediction using medical imaging. In this work, we particularly focus on the GCN method for analyzing the neuroimages of brain disorders prediction in an end-to-end fashion.

Another line of effort aims to learn the dynamic FC analysis rather than the stationary. Dynamic functional connectivity analysis provides valuable information for understanding functional brain activity underlying different cognitive processes [11], [12]. Recent studies have shown that exploring spatial and temporal features of the brain network is vital for fMRI image classification. Two recent papers [13], [14] were the first work to consider both the spatial and temporal features of the brain network for capturing the spatio-temporal dynamics. A spatial-temporal graph convolutional network (ST-GCN) is proposed for brain network [13]. Each spatial-temporal graph convolutional layer constructs spatial characteristics with a graph convolutional operator and models temporal dynamic with a convolutional operator. An end-to-end deep neural network with combining temporal convolutional networks (TCNs) and GCNs to learn both the spatial and temporal components in rs-fMRI. However, although both works consider the dynamic signal information, the network is still static without considering the dynamic variation of structure information of the brain network. For temporal dynamics of brain network modeling, both signals of each brain region and global topological correlation among the brain regions are very important for brain network analysis. However, most existing deep learning works applied to rs-fMRI analysis fail to consider both aspects simultaneously. Therefore, how to effectively model discriminative spatial-temporal features and preserve the graph structures is still a challenging problem. Another problem in dynamic brain network modeling is the presence of noisy correlations in the brain network. The presence of noise in brain images is owing to the fact that measurement errors are likely to arise due to technological limitations, operator performance, equipment, environment, and other factors [15]. Moreover, the correlation is not reliable by Pearson's correlation, which is the simplest and most widely used method but restricted to linear associations and is overly sensitive to outliers [16]. Furthermore, from the clinical perspective, identifying biomarkers would be more crucial to different brain disorders. The prediction accuracy, as well as reliable and explainable biomarkers, remain the key focus of brain network research. Therefore, it is essential to design a unified framework to jointly eliminate the noisy connections in dynamic FCs and spatial-temporal brain network feature learning, which can model the temporal dynamics of network structures. To overcome those shortcomings, we formulate functional connectivity networks with spatio-temporal graphs and propose a temporal graph representation learning for brain networks by exploiting graph-temporal information, named BrainTGL. At first, we incorporate multi-graph clustering into GCN model to enhance the important connections and remove the irrelevant connections with a supervision scheme. The multi-scale brain network construction combined with cluster-

ing could generate more robust and biologically meaningful functional connectivity networks. To concurrence modeling the dynamic information, we proposed a dual temporal graph learning LSTM module to deal with complex dynamic associations by capturing the spatio-temporal features in the spatio-temporal consistent coarsen brain networks and extracting an embedding rich in spatio-temporal features. There exists a co-occurrence relationship between spatial and temporal domains. The module of DTG-LSTM involves 1) convolutional layer for brain region temporal feature learning; 2) graph structure aware LSTM, which merits both GCN and LSTM, node feature learning with neighbors across the multiple time windows. Furthermore, a recurrent-skip component is introduced to extend the temporal span of the information flow and hence ease the optimization process. It can not only effectively capture discriminative features in temporal signal dynamics but also explore the temporal graph correlation. We also present a multi-window scheme to increase temporal receptive fields of the BrainTGL, which boosts the ability to learn the different level temporal representation. Extensive experiments on two real medical clinical applications: gender classification on the HCP dataset [17] and diagnosis of ASD on the ABIDE dataset [18], demonstrating the advantage of the proposed framework. The extensive experimental results suggest that temporal graph representation learning for brain networks by incorporating the multi-graph consistent clustering and dual temporal graph learning LSTM can improve prediction performance.

II. RELATED WORK

Many efforts have been devoted to automated brain diagnosis or Gender diagnosis based on rs-fMRI. Existing works are mainly divided into two branches: static brain network analysis and dynamic brain network analysis.

A. Static brain network analysis methods

The construction of static functional connectivity networks is generally based on pair-wise temporal correlation between different brain regions' BOLD signals. Conventional methods are usually based on the assumption that FC is stationary within the entire scan period. For example, Jie *et al.* [5] introduced a graph-kernel based method that identified MCI patients from normal controls by designing a measure to compute the topological similarity between the functional connections. The major disadvantage of these methods is that feature extraction of brain networks and classification are treated as two independent tasks, hindering the final performance.

Many efforts have been devoted to incorporating network-based feature learning and classifier training into a unified framework to address this problem. Kudo *et al.* [19] proposed to extract the network representation by exploiting the subgraphs from each network and adopted a boosting algorithm to enhance network classification. Cao *et al.* [20] developed an end-to-end tensor-based brain network embedding method for anxiety disorder prediction. Eslami *et al.* [7] proposed a joint learning method combining an autoencoder with a single layer perceptron (SLP) for automated diagnosis of Autism Spectrum

Disorder (ASD). Some work has recently introduced the GCN model to learn the brain network embedding considering the network topology information. Yao *et al.* [6] proposed a multi-scale triplet graph convolutional network (MTGCN) for brain functional connectivity analysis derived from rs-fMRI data. They constructed multi-scale FCs for each subject by employing multi-scale templates at first. Then a triplet GCN model is developed to learn multi-scale graph representations of brain networks with a weighting scheme for final prediction. By analyzing stationary FC, these conventional methods have shown potential advantage in understanding the functional abnormalities caused by some brain diseases by analyzing stationary FC. However, these methods fail to model the temporal dynamics in rs-fMRI.

B. Dynamic brain network analysis methods

Recently, growing evidence suggests that FC is not stationary [11], [12]. The dynamic FC properties can more reliably monitor the changes of macroscopic neural activities underlying cognitive and behavioral decline, which results in many efforts shifted toward dynamic FC analysis. Existed work can be divided into two main directions: signal-level dynamic FC analysis and graph-level dynamic FC analysis.

1) *Signal-level dynamic FC analysis*: One active area of research is signal-level dynamic FC analysis. Most works focus on capturing temporal dynamics on the signal level, whereas the FC in the brain network is still stationary. These methods are not able to model the relationship among the dynamic graphs. A combination of GCN and CNN is performed on the spatio-temporal graph to capture the spatio-temporal dynamics with a fixed graph structure [13], [14]. For example, Gadgil *et al.* [13] proposed a concept of spatio-temporal graphs to formulate the rs-fMRI data. They then developed a spatio-temporal graph convolutional network (ST-GCN) to model the temporal dynamics of functional connectivity and learn the graph edge importance. Azevedo *et al.* [14] proposed an end-to-end framework via GNN and TCN to capture the spatio-temporal features. Unlike ST-GCN [13], they regarded the whole BOLD time series as input and employed GNN to learn node features and edge features alternatively for a better graph-level embedding.

2) *Graph-level dynamic FC analysis*: Another active research area is graph-level dynamic FC analysis that focuses on capturing the graph-level temporal features of dynamic FC networks. For example, Monti *et al.* [21] proposed a smooth, incremental graphical lasso estimation (SINGLE) algorithm that took fMRI time-series data as inputs to infer dynamic brain networks for each subject. They introduced a l_1 -norm regularizer to enforce the sparsity of the network and used a temporal homogeneity regularizer (via a l_1 -norm-based extension of the fused Lasso regularizer) to penalize the difference between consecutive networks. Cai *et al.* [22] proposed to employ a time-varying graphical lasso (TVGL) model to estimate dynamic FCs using an element-wise penalty (*i.e.*, $l_{log,1}$ -norm) to enforce sparsity in the FC matrix and an Laplacian penalty to inject the similarity between adjacent time-stamps. However, the methods mentioned above are all

designed for brain network construction with dynamic FCs. Furthermore, some work applied the dynamic brain network to the diagnosis of diseases. For example, Wee *et al.* [23] proposed a fused Lasso based sparse learning algorithm to infer dynamic FCs and diagnose mild cognitive impairment jointly. Jie *et al.* [24] developed a manifold regularized multi-task feature learning framework to extract discriminative features from the dynamic FCs, and employed a multi-kernel SVM to diagnose Alzheimer's disease. However, these methods treat network-based feature extraction and classification as two independent steps, leading to sub-optimal performance of brain disease classification. Few works have been dedicated to incorporating network-based feature learning and classifier training into a unified framework. For example, Wang *et al.* [25] proposed an end-to-end temporal dynamics learning (TDL) method for diagnosis of brain disease based on dynamic FCs. They first transformed rs-fMRI time series into dynamic FCs using overlapping sliding windows and then introduced a group-fused Lasso regularizer to capture the global temporal dynamics of these networks.

Although most existing dynamic brain network analysis methods mentioned are able to model both spatial and temporal features simultaneously, there are still some drawbacks: 1) All of them only consider either signal-level temporal dynamics or graph-level temporal dynamics, failing to consider both of them simultaneously; 2) They also ignore the noisy correlations within each brain network and the inconsistency across brain networks.

III. METHOD

This section first introduces the problem statement of our tasks and then presents the proposed BrainTGL in detail.

A. Problem statement

In this paper, we are interested in the task of automated diagnosis with rs-fMRI time-series data. Rs-fMRI time-series data can be seen as a multivariate time series, in which each ROI corresponds to a variable and has a corresponding time-series signal. More formally, given rs-fMRI time-series data $X = \{x_1^{(i)}, x_2^{(i)}, \dots, x_n^{(i)}\}_{i=1}^N$ and their corresponding labels $Y = \{y_1, y_2, \dots, y_N\}$ where $x_j^{(i)} \in \mathbb{R}^m$, $j \in \{1, 2, \dots, n\}$, $y_i \in \{-1, 1\}$, m is the variable dimension, n is the number of ROIs, and N is the number of subjects in the dataset, we aim at learning a mapping function $f : X \rightarrow Y$, which maps the rs-fMRI time-series its corresponding label.

B. Construction of Temporal Multi-graph in Brain Network

Recently, growing evidence suggests that fMRI time-series data contains plenty of temporal information. However, several pioneering studies devoted to automated ASD diagnosis are based on static brain function network analysis, ignoring temporal information in fMRI time-series data. It has been proved that using spatial information with the assistant of time information can improve the task's performance [26], [27]. As a result, we assume that the temporal information in fMRI

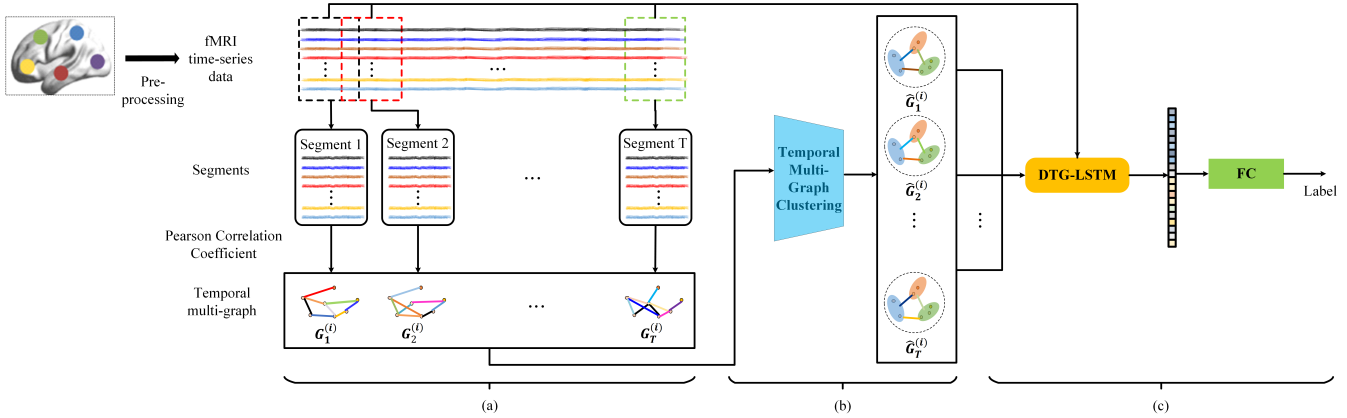


Fig. 1: The overall architecture of our proposed BrainTGL. (a): The construction of the temporal multi-graph contains two steps. The fMRI time-series data of each subject is first partitioned into a series of time-series segments. A graph (brain network) is constructed on each each segment with PCC. Finally, we obtain the corresponding temporal multi-graph for each subject. (b): With the constructed temporal graph series, we propose a temporal multi-graph clustering to eliminate noisy edges in temporal multi-graphs and achieve a temporal supergraph series which are consistent for all the subjects by sharing the clustering parameter. (c): A Dual temporal graph learning LSTM (DTG-LSTM) is proposed to sufficiently model the spatio-temporal patterns of the temporal supergraph series from the BOLD signals level and graph level ,respectively.

time-series data benefits the automated diagnosis task, based on which we adopt the idea of spatio-temporal dependency modeling.

To capture the spatio-temporal dependency, we introduce a spatial-temporal graph structure, the temporal multi-graph. Temporal multi-graph, as the name implies, is a kind of graph sequence that has a dependence on the time dimension. We first formally define the temporal multi-graph for each subject. Let $\mathcal{D} = \{G_t^{(1)}, G_t^{(2)}, \dots, G_t^{(N)}\}_{t=1}^T$ denote temporal multi-graphs of a dataset, where each sample is indicated as a sequence of networks, T is the number of rs-fMRI time-series segments, and N is the number of subjects. All networks share the same brain region set of vertices V where each vertex corresponds to a specific brain region. The $G_t^{(j)}$ defined at the t -th segment for the j -th subject can be represented by an adjacency matrix $A_t^{(j)} \in \mathbb{R}^{n \times n}$, where n is the number of ROIs, reflecting the connectivity strength between paired ROIs. Based on this concept, we then build a temporal multi-graph for each subject in a dataset.

The construction of temporal multi-graph is illustrated in Fig. 1 (a). The input of this block is rs-fMRI time-series data. We assume that the fMRI time-series data for i -th subject is $X_i = (x_1^{(i)}, x_2^{(i)}, \dots, x_n^{(i)})^T \in \mathbb{R}^{n \times m}$ where n represents the number of region of interests (ROIs) and each vector $x_j^{(i)} \in \mathbb{R}^m$ ($j = 1, 2, \dots, n$) in X_i represents the BOLD signal series of the j -th ROI. Based on fMRI time-series data X_i , we construct the temporal multi-graph for i -th subject consisting of two steps, including the partition of fMRI time series and the construction of graph series.

1) Partition of fMRI Time Series: To better characterize the temporal variability of the functional connection associated with a set of given regions, we use sliding window technology to segment fMRI time-series data into T overlapping windows of constant size \mathcal{L} . Specifically, we set a window with a const size \mathcal{L} , and then roll it on the fMRI time-series data with

a constant stride \mathcal{S} . We then obtain a sequence of T time-series segments. For each subject, a sequence of T time-series segments will be treated as the input of the next step.

During the above procedure, there is an important factor called overlap ratio in the sliding window method which represents the degree of overlap between two adjacent windows. Formally, we define $R = \mathcal{L}/\mathcal{S}$ as the overlap ratio during the window sliding. The smaller the R is, the less redundant but weak information exists in temporal multi-graph. On the contrary, the bigger the R is, the more redundant but sufficient information exists in temporal multi-graph. An appropriate R helps to mine the temporal information between graph structures. In our experiment, this is a hyper-parameter that has a significant impact on the performance of our model.

2) Graph Series Construction: The strength of the functional connection of the brain network is often measured by the strength of the correlation between the BOLD time-series of each ROI. Many methods such as pearson correlation coefficient (PCC), covariance correlation coefficient, etc. are used to calculate the correlation between time series. In this article, we adopt PCC to calculate the correlation between ROIs. Each vertex v_i represents a brain region, and the corresponding time series is indicated as x_i . PCC between the time series x_i at the vertex v_i and x_j at the vertex v_j is given by

$$r_{ij} = \frac{\text{cov}(x_i, x_j)}{\sqrt{\text{cov}(x_i, x_i) * \text{cov}(x_j, x_j)}} \quad (1)$$

where $\text{cov}(x_i, x_j)$ represents the covariance of time series x_i and x_j .

We calculate the correlation between each pair of brain regions for each segment. Then, a series of dynamic graphs are generated.

C. Temporal multi-graph clustering

We convert fMRI time-series data into temporal multi-graph by temporal multi-graph construction block. However, the

multi-graph time series constructed in the above procedure still has two problems. Firstly, the high noisy connection in the brain network leads to poor classification performance. Secondly, there exist inconsistencies in the subjects from multi-sites. Many works based on static brain network analysis have made a great effort to eliminate the inconsistency among the subjects from multi-sites. However, the inconsistency in the dynamic brain network introduces a more significant challenge to our classification task. Therefore, it's essential to eliminate the inconsistency in dynamic FCs.

In our work, we employ graph clustering to remove the noisy edges in the brain network and obtain consistent and clean graph structures at the same time [28]. However, the traditional clustering methods are unsupervised as independent procedures before the classification. Therefore, in our work, we apply the multi-graph clustering method on the dynamic brain network, which removes the noisy correlation in the brain network by considering the group-level consistency in the subjects from multi-sites. Moreover, we employ a unified framework to jointly train the proposed multi-graph clustering and temporal graph embedding for classification in a supervision scheme, which leads to an improved quality of clusterings and graph embedding.



Fig. 2: The illustration of nodes clustering for supergraph

The general idea of the method is to group the nodes of an original graph into some clusters with the rule of hiding the non-indicative edges and highlighting the indicative edges, illustrated in Fig. 2. Given an original graph $G = \{V, A\}$, $A \in \mathbb{R}^{n \times n}$ denotes the corresponding adjacency matrix of G , and $V = \{v_1, v_2, \dots, v_n\}$ represents the set of nodes in G , the aim is to transform an original graph G into a hypergraph $\hat{G} = \{\hat{V}, \hat{A}\}$ with a coarsened structure, where \hat{V} denotes the set of supernodes in \hat{G} , $\hat{A} \in \mathbb{R}^{c \times c}$ denotes the corresponding adjacency matrix of \hat{G} , and c denotes the number of supernodes. We introduce a learnable parameter $F \in \mathbb{R}^{n \times c}$. F indicates the membership of a node to a cluster. With the optimized F , we can obtain a set of clusters as supernodes $\hat{V} = \{SN_1, SN_2, \dots, SN_c\}$ and the weighted adjacency matrix of the supergraph: $\hat{A} = F^T AF \in \mathbb{R}^{c \times c}$. A coarsened graph \hat{G} highlighting the notable edges in original graph G is constructed with the supernodes $\hat{V} = \{SN_1, SN_2, \dots, SN_c\}$ and the weighted adjacency matrix \hat{A} .

We assume each node v_i has its corresponding score s_i which represents its importance in graph G . Furthermore, with the node importance of s_i and s_j , we define the importance of edge e_{ij} as $s_i * w_{ij} * s_j$, where w_{ij} denotes the weight of edge e_{ij} . The learned edge weight help us identify the indicative edges. The weight of the superedge between supernodes SN_f

and SN_f then represents as

$$W_{ef}^{SN} = \sum_{i \in SN_e \wedge j \in SN_f} s_i * w_{ij} * s_j \quad (2)$$

Briefly, the superedge between supernode e and supernode f is the aggregation of edges multiplying with node importance. Then F can be formally defined as

$$F_{ij} = \begin{cases} s_i, & i \in SN_j \\ 0, & i \notin SN_j \end{cases}$$

To train our temporal multi-graph clustering with a supervision scheme, we collaborate the node clustering with the graph convolution for a supervision scheme classification. To constrain the consistency of temporal multi-graph, we further perform multi-graph clustering on all graph structures with a shared F . By optimizing the learnable F , we can obtain an optimal multi-graph clustering result. At the same time, we can finally identify the indicative edges for our task.

During the supervised learning, there exist many problems. To avoid the occurrence of negative value, we perform a ReLU operation on the trainable real-valued matrix F to generate a non-negative matrix, which represent as $\tilde{F} = \text{ReLU}(F)$, and then the output of the temporal multi-graph clustering becomes $\hat{A} = \text{ReLU}(\tilde{F})A\text{ReLU}(\tilde{F})$. However, the negative values initialized in the matrix F will not be updated later for their gradients are zero. To address this problem, we use a l_1 -norm regularizer to penalize the negative values, which can represent as $L_{neg} = \sum_{i=0}^N \sum_{j=0}^C \text{ReLU}(-F_{i,j})$. Since the result of clustering requires that the nodes between different clusters do not overlap, we add an orthogonal constraint $L_{rec} = \sum_{i,j=0 \wedge i \neq j}^C ((F^T F)_{i,j})^2$ to hinder the overlap. To balance the group sizes for a better interpretability, we further introduce the balance loss: $L_{var} = \text{Var}(\text{diag}(F^T F))$, where $\text{Var}(\cdot)$ means variance.

Unlike traditional clustering that assigns nodes based on similarity, temporal multi-graph clustering hides the noisy connectivity by grouping nodes into a supernode, thus highlighting the indicative edges connecting to supernodes. Another advantage of our temporal multi-graph clustering is to treat clustering and classification as a whole by collaborating the graph clustering with temporal graph embedding learning in a supervision scheme.

D. Dual temporal graph learning LSTM

To sufficiently model the spatio-temporal patterns of brain activity, we propose a spatio-temporal modeling method called dual temporal graph learning LSTM (DTG-LSTM) to fully learn temporal characteristics in fMRI data from two aspects: one-dimensional BOLD signals and multivariable temporal graphs, which is quite different from the prior work. Fig. 3 (a) illustrates the pipeline of DTG-LSTM.

We first design a signal representation learning (SRL) block for learning the temporal features from the BOLD signal of each node as the corresponding node initial embedding via a stack of convolutional layers illustrated in Fig. 3 (b). The

embedding of node (ROI) of each graph is learned after l steps of convolutional layers as follow:

$$e^{\mathcal{S}^{(l+1)}}(u) = \sum_{s=0}^{U-1} e^{\mathcal{S}^{(l)}}(u-s) * \mathcal{K}^{(l)}(s) \quad (3)$$

where $\mathcal{K}^{(l)}$ is a convolutional kernel of l -th layer with a kernel size of U and u denotes the elements in BOLD signal.

We then design a GSA-LSTM to capture spatio-temporal features at the graph level. GCN is a very effective deep learning framework for exploring spatial domain information. However, it's not capable of capturing temporal characteristics. To address this problem, we propose a block to incorporate the graph convolution into the LSTM to capture the spatio-temporal features for modeling dynamic brain networks effectively. Due to gradient vanishing, LSTM usually fails to capture a long-term correlation. We propose to alleviate this issue via a recurrent-skip component that leverages the periodic pattern in real-world sets. To alleviate it, we develop a recurrent structure with temporal skip connections to extend the information flow's temporal span and ease the optimization process. Specifically, a skip-connection is added between the currently hidden cell and the hidden cells in the same phase in adjacent periods.

The GSA-LSTM block is illustrated in Fig. 3. The input of this block is the temporal coarsened multi-graph with node embedding, as shown in Fig. 1 (c). The structure of the GSA-LSTM cell is shown in Fig. 3 (c). The GSA-LSTM has three gates the same as traditional LSTM: the input gate, the forget gate, and the output gate. However, the operation of each gate is instead a stack of graph convolutional layers to capture the spatial features of the graph structures. The input of the GSA-LSTM cell has three parts: H_{t-p} , A_t and E_t^G , where H_{t-p} denotes the hidden state obtained in $(t-p)$ -th step, p is the number of hidden cells skipped through, \hat{A}_t is the adjacency matrix of t -th graph structure in the input graph series and E_t^G is the corresponding features of the t -th graph structure in the input graph series. Unlike traditional LSTM based on vectors, the input \hat{G}_t , hidden state H_{t-p} , and cell memory C_t of GSA-LSTM are all graph-structure. The updating process can be formulated as

$$I_t = \sigma(W_{xi} * f_{gcn}(\hat{G}_t) + W_{hi} * f_{gcn}(H_{t-p}) + b_i) \quad (4)$$

$$F_t = \sigma(W_{xf} * f_{gcn}(\hat{G}_t) + W_{hf} * f_{gcn}(H_{t-p}) + b_f) \quad (5)$$

$$O_t = \sigma(W_{xo} * f_{gcn}(\hat{G}_t) + W_{ho} * f_{gcn}(H_{t-p}) + b_o) \quad (6)$$

$$U_t = \text{ReLU}(W_{xc} * f_{gcn}(\hat{G}_t) + W_{hc} * f_{gcn}(H_{t-p}) + b_c) \quad (7)$$

$$C_t = \text{Tanh}(I_t * U_t + F_t * C_{t-p}) \quad (8)$$

$$H_t = O_t * \text{Tanh}(C_t) \quad (9)$$

where $f_{gcn}(\cdot)$ represents a graph convolution operation. Note that the E_t^G is graph embedding of \hat{G}_t . The graph convolution for l -th layer can be formulated as

$$E_t^{G^{(l+1)}} = \text{ReLU}(A_t E_t^{G^{(l)}} W^{(l)}) \quad (10)$$

where $W^{(l)}$ is a trainable weight matrix of l -th layer, $E_t^{G^{(l+1)}}$ are the node embeddings computed after l steps of the GCN

and the node embeddings $E_t^{G^{(l)}}$ are generated from the previous message-passing step. Noting that $E_t^{G^{(0)}}$ is the graph initial embedding of \hat{G}_t which is equal to E_t^S , each item of which is obtained by Eq (3).

Then we combine the outputs of GSA-LSTM to produce a final embedding as follow:

$$\hat{H}_t^C = W^R H_t^R + \sum_{j=1}^p \sum_{i=1}^j W_i^S H_{t-i}^S + b \quad (11)$$

where H_t^R is the hidden state of recurrent-component at time stamp t , $H_{t-p+1}^S, H_{t-p+2}^S, \dots, H_t^S$ are denoted as the p hidden states of recurrent-skip component from time stamp $t-p+1$ to t , W^R and W_i^S are learnable matrices.

Finally we flatten \hat{H}_t^C into a vector along the node dimension and finally feed it into a linear layer for classification.

E. Ensemble

The hyperparameter of window length influences the performance of our algorithm. Motivated by this, we need to find an appropriate value to eliminate the interference of the inferior temporal multi-graph. It is time-consuming to find an optimal solution. To alleviate it, we adopt a multi-time window ensemble strategy. As shown in Fig. 4, we train multiple BrainTGLs on the temporal multi-graph with different window lengths. Finally, these trained models are combined to achieve a final prediction with the voting scheme.

F. Data augmentation

To solve the issue of insufficient data, we adopt a data augment scheme. Specifically, we divide the full sequence of each subject into several sub-sequence of length m^s without overlap. During the training stage, we take all the sub-sequence of each training subject to train the model. At the testing stage, we apply the trained BrainTGL on each sub-sequence, and the prediction values are combined to produce a final subject-level prediction with a voting scheme.

IV. EXPERIMENT

A. Datasets and Evaluation Protocols

1) Datasets: We evaluated our proposed model on two challenging benchmarks for binary classification tasks: ABIDE database (Autism Brain Imaging Data Exchange database) and HCP database (Human Connectome Projects database).

ABIDE: ABIDE database collected 1112 subjects, including 539 individuals with ASD and 573 typical controls (ages 7-64 years, median 14.7 years across groups) from different 17 acquisition sites. We used data from the ABIDE pre-processed connectome project (PCP) data preprocessed by the Configurable Pipeline for the Analysis of Connectomes (CPAC). The detailed procession of PCP and CPAC can be referenced in [29]. After the preprocessing, we obtained 871 quality MRI images with phenotypic information, comprising 402 individuals with ASD and 464 normal controls acquired at 17 different sites. We further selected 512 individuals whose

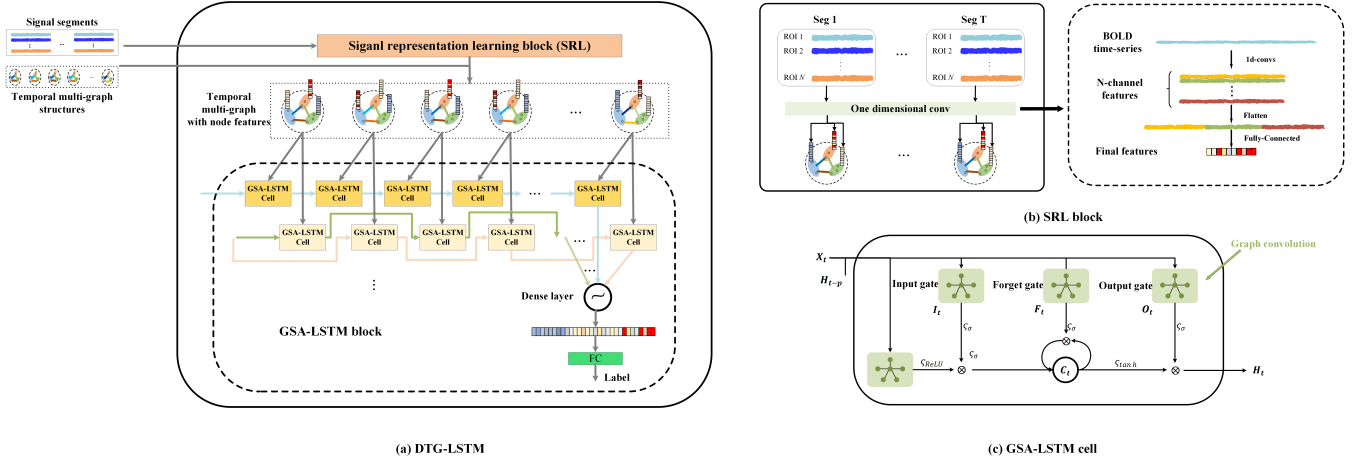


Fig. 3: The illustration of our proposed DTG-LSTM module.

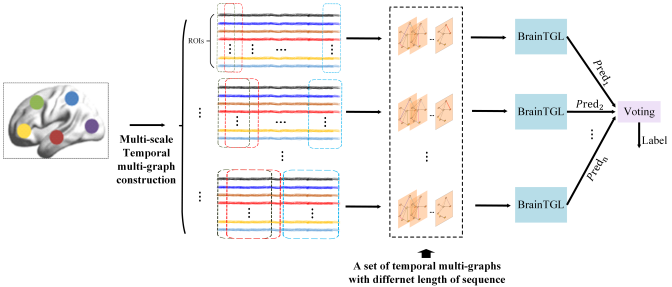


Fig. 4: An ensemble of BrainTGL with multiple window parameters for sliding windows.

sequence length of ROIs' corresponding BOLD time-series is between [196, 250].

HCP: Human Connectome Project (HCP) S1200 contained the rs-fMRI data for 1096 young adults (ages 22–35). We used the first session (15 min, 1200 frames, TR=0.72s) for each subject and excluded five rs-fMRIs with less than 1200 frames, resulting in the data of 498 females and 593 males. Each rs-fMRI went through the minimal processing pipeline with fMRI Surface algorithm [30], which mapped each volume time series to the standard CIFTI grayordinates space. The cortical surface was parcellated to 22 major ROIs.

2) Evaluation metrics: In our experiments, we chose four metrics, *i.e.*, classification accuracy (ACC), the area under the receiver operating characteristic (ROC) curve (AUC), sensitivity (SEN), and specificity (SPE), to evaluate the performance of our proposed method. We employed a 5-fold cross-validation strategy to evaluate the performances.

B. Comparison with the State-of-the-art Methods

To validate the effectiveness of our proposed method on the binary classification on the fMRI time-series data, we compared our proposed method with several current state-of-the-art methods on ABIDE and HCP as follow:

GroupINN [8] is an end-to-end neural network-based method combining the multi-graph clustering with the graph convolutional network.

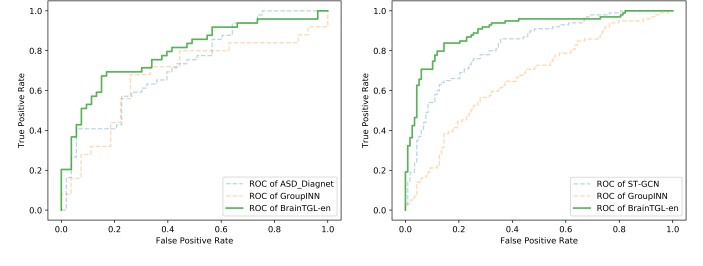


Fig. 5: The ROC of multiple computing methods.

ASD DiagNet [7] is a joint learning method combining an autoencoder with a single layer perceptron (SLP) to improve quality of extracted features and optimized parameters for the classification model. In this method, we employ the same autoencoder structure as described in [7].

Eigen Pooling GCN [31] is a joint learning method combining an end-to-end trainable graph pooling with server GCNs to produce hierarchical representations of graphs.

ST-GCN [13] is a joint learning method combining CNNs with GCNs to model the spatio-temporal dependency in fMRI data.

CNN+GCN [14] is a joint learning method combining CNNs with GCNs to model the spatio-temporal dependency in fMRI data. Different from Gadgil *et al.* [13], they replace CNNs with TCNs and use a graph network (GN) framework [32] which learns node embedding and edge embedding alternately to produce representations of graphs.

The results of the comparisons in the binary classification tasks are reported in Table I. The ROC curves in the binary classifications tasks are further plotted in Fig. 5. We can see that our methods can consistently and substantially outperform the previous brain network classification methods on both tasks. Our final method BrainTGL-en obtained an accuracy of 69.3% and 81.0% on both datasets, respectively. It can be seen that our model can achieve a comparable performance without an ensemble scheme with the accuracy on ABIDE and HCP are 65.2% and 79.2%, respectively.

TABLE I: Performance comparison of various methods on HCP dataset and ABIDE dataset.

Dataset	Method	AUC(%)	ACC(%)	SEN(%)	SPE(%)
HCP	GroupINN	61.2	58.6	23.4	88.3
	Eigen_pooling	67.9	68.7	73.8	71.0
	ST-GCN	86.5	78.1	71.8	83.5
	CNN+GCN	64.6	60.9	57.1	64.1
	BrainTGL	86.1	79.2	73.5	83.9
ABIDE	BrainTGL-en	88.4	81.0	76.0	85.3
	ASD DiagNet	66.2	66.6	57.3	75.2
	GroupINN	64.7	63.4	62.4	64.4
	ST-GCN	50.0	51.9	50.0	50.0
	BrainTGL	67.8	65.2	64.6	65.8
	BrainTGL-en	74.0	69.3	67.4	71.1

Specifically, existing methods that only incorporate spatial graph convolution (including GroupINN and Eigenpool GCN) often pay more attention to the spatial features from the data. They usually transform the fMRI time-series data into a brain network and perform a GCN network to extract spatial domain features, thereby potentially losing abundant temporal information in the BOLD time series. Therefore, they have limited performance of classification. As for ASD-DiagNet, they use the PCC to convert the time series signal into a brain network. Then, they flatten the correlation matrix and put the result into a fully connected network for representation learning. These two methods are focused on mining the global features from a brain network, unable to provide interpretability essential in neuroscience research. At the same time, the FC operation is computationally expensive. Compared with the other spatio-temporal modeling methods (including CNN+GCN and ST-GCN), our proposed method achieved better results on both datasets. The main reason can fall into there aspects: 1) they both ignore the inconsistency of brain networks between subjects, which makes a significant challenge to learn a good representation; 2) They are still focused on static brain network analysis, which provides limited opportunity to capture the temporal dynamics fully; 3) they only consider the signal-level temporal dynamics ignoring the graph-level temporal dynamics.

In summary, compared to existing methods, our proposed methods jointly consider the potential relations of different regions of the brain in both spatial dimension and temporal dimension, which can provide more discriminative and robust information and is able to perform end-to-end training. These experimental results validate the superiority of our method.

C. Experiment on Other Parcellations

From the analysis of the results shown above, we conclude that our proposed method achieved better performance compared to other methods. To test whether the above observations were dependent on the choice of the atlas, we applied the same methodology on different atlases. We evaluated our model on three other structural atlases besides CC200. They are Talairach Daemon (TT) atlas (derived from myeloarchitectonic segmentations), Harvard-Oxford (HO) atlas (derived from anatomical landmarks: sulci and gyral), Eickhoff-Zilles (EZ) atlas (derived from cytoarchitectonic segmentations), and Automated Anatomical Labeling (AAL) atlas (derived from

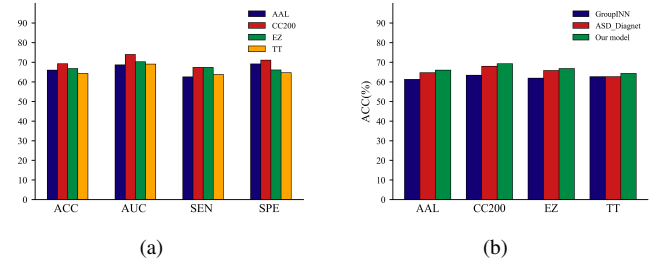


Fig. 6: Performance of our model and the comparable methods on multiple atlases

structural criteria). The performance of our model BrainTGL-en on multiple atlases is presented in Fig. 6 (a). From Fig. 6 (a), we find that BrainTGL-en on CC-200 atlas yielded the best performance in terms of all the metrics, which implies that the pairwise correlations among CC-200 regions contain more discriminatory patterns than other atlases. Furthermore, to validate the superiority of the dynamic brain network, we selected two state-of-art methods including ASD Diagnet and GroupINN, on the static brain network and compared them on these atlases. The results are shown in Fig. 6 (b). Our proposed BrainTGL-en achieved higher accuracy than the previous methods. Therefore, we conclude that the analysis of dynamic brain networks is better than the one on a static brain network.

D. Ablation Study

1) *The Impact of Modules:* To demonstrate the efficiency of our framework design, a careful ablation study was conducted. Specifically, the comparison was conducted between our method and the intermediate method or basic method with a single component or a combination of multiple components.

The experimental results are reported in Table II. Our systematic study on HCP dataset suggests the following trends:

1. C-DTG-LSTM-aug-en (our model) yielded the best performance with respect to all the metrics, demonstrating our proposed components' advantage. All the components of Brain-TGL together lead to the robust performance of our approach on all the metrics.

2. GCN-LSTM shows the worst performance among the algorithms for all metrics, even worse than GCN. However, the result does not indicate the effectiveness of the LSTM, since the GCN-LSTM model does not appropriately capture the dynamic pattern in fMRI data well, which loses discriminative and robust temporal information.

3. We can see that DTG-LSTM achieves better results than GCN-LSTM, which demonstrates that the temporal relations and structural relations are complementary and achieves a conclusion that a simple LSTM module can not capture the temporal information in fMRI data well. By adopting a dual temporal learning method, we can take advantage of the temporal information to improve classification performance.

4. By comparing DTG-LSTM-aug and DTG-LSTM, it can be clearly observed that the insufficient number of samples in the dataset is one of the main factors hindering the

TABLE II: Ablation study on HCP dataset and ABIDE dataset.

Dataset	Method	GCN	LSTM	Clustering	Augmentation	DTG-LSTM	Ensemble	ACC(%)	SEN(%)	AUC(%)	SPE(%)
HCP	GCN	✓						59.0	62.2	58.6	55.1
	GCN-LSTM	✓	✓					58.3	60.5	57.4	54.8
	DTG-LSTM					✓		71.3	71.3	71.0	70.8
	DTG-LSTM-aug				✓	✓		73.7	64.4	81.8	81.4
	DTG-LSTM-aug-en				✓	✓	✓	75.4	67.9	83.1	81.7
	C-DTG-LSTM-aug			✓		✓		79.2	73.5	86.1	83.9
	C-DTG-LSTM-aug-en			✓	✓	✓	✓	81.0	76.0	88.4	85.3
ABIDE	GCN-LSTM	✓	✓					58.4	59.1	58.8	57.1
	C-GCN-LSTM	✓	✓	✓				60.3	55.7	63.8	64.7
	C-DTG-LSTM			✓			✓	65.2	64.6	67.8	65.8
	C-DTG-LSTM-en			✓			✓	69.3	67.4	74.0	71.1

TABLE III: Ablation study on recurrent-skip component and combination of GCN and LSTM on HCP dataset

Method	ACC(%)	SEN(%)	SPE(%)	AUC(%)
BrainTGL w/o recurrent-skip component	74.3	77.4	71.7	85.2
BrainTGL	79.2	73.5	83.9	86.1
BrainTGL (GCN+LSTM)	76.6	73.7	79.0	85.1
BrainTGL (GSA-LSTM)	79.2	73.5	83.9	86.1

performance of our model. The data augmentation facilitates the learning of the dynamic brain network and improves the discrimination capability of deep learning models.

5. Results show that the ensemble strategy provides improved performance without the need to determine an efficient method to eliminate its determination of the window size.

6. Additionally, we can see that C-DTG-LSTM-aug-en achieved better results than DTG-LSTM-aug-en, confirming that temporal multi-graph clustering plays a crucial role in modeling dynamic brain networks. It can effectively eliminate the noise edges in the original time series multi-graph and reduce the inconsistency of graph structures of subjects from multi-sites.

From the study on ABIDE dataset, we can make similar observations and conclusions.

2) *The Impact of recurrent-skip component*: To verify the impact of the skip-connection component we proposed, we conduct an ablation study on the HCP dataset. The experimental results are reported in Table III. We can see that the skip-connection trick increases the performance by 4.9% on the HCP dataset, indicating the effectiveness of skip-connection. The introduction of recurrent-skip component is able to boost the model performance of the GSA-LSTM, showing that the recurrent-skip component is helpful to better model long and short-term temporal patterns in fMRI data.

3) *The impact of the combination of GCN and LSTM*: To justify the effectiveness of our GSA-LSTM design, a careful ablation study is conducted. We compared BrainTGL(GSA-LSTM) with a simple combination of GCN and LSTM named BrainTGL(GCN-LSTM), where a series of temporal graph embeddings are obtained by GCN and then fed into the LSTM without preserving the graph structure. The observation implies the usefulness of the proposed appropriate combination, which validates our motivation that incorporating graph convolution into LSTM with considering the dynamic graph structure variation is able to model the spatio-temporal dependency.

E. Interpretability

Although deep neural networks are usually regarded as black boxes, in this paper, we attempt to improve explainability by identifying the critical subnetwork through the indicative edges learned. For instance, we can visually explore the temporal coarsened multi-graph generated by the temporal multi-graph clustering module and compare them with the original temporal multi-graph. We selected three samples, including one patient with ASD and two normal controls, and visualized their original brain network and coarsened brain network, respectively. The results are presented in Fig. 7. By observing them individually, the original graphs of each subject showed high inconsistency over the time series. However, the inconsistency of each object is alleviated with the process of temporal multi-graph clustering. Therefore, our results seem to yield solid evidence that imposing a temporal multi-graph clustering method during training the network is a viable method for improving GCN's performances for diagnosis. We can also find that most of the edges in the brain network are non-indicative of the final classification task. Through temporal multi-graph clustering, the indicative edges are highlighted. Furthermore, by comparing the results in Fig. 7 (a) and Fig. 7 (b), it is apparent to see that the difference between the original graph of ASD individuals and Normal controls is difficult to be differentiated. By contrast, the difference between ASD individuals and Normal controls with respect to the coarsened graphs is strengthened by the temporal multi-graph clustering. By comparing Fig. 7 (a) and Fig. 7 (c), we can also see that temporal multi-graph clustering weakens the heterogeneous of the dynamics brain network between subjects belonging to the same class. By strengthening the difference between individuals from different classes and weakening the difference between individuals from the same class, the temporal multi-graph clustering further improves the performance of our classification.

Moreover, our method can reveal the subnetworks that are most informative to the final prediction. Our subnetwork analysis is also based on our clustering parameter F . As introduced in chapter 3.3, each item $F_{i,j}$ in F can be interpreted as the membership of the node i to the cluster SN_j . With the optimized F , the score of the p -th subnetwork S_p is calculated as

$$score_p = \sum_{i,j \in S_p \wedge i \in SN_e \wedge j \in SN_f \wedge e \neq f} F_{i,e} * F_{j,f} \quad (12)$$

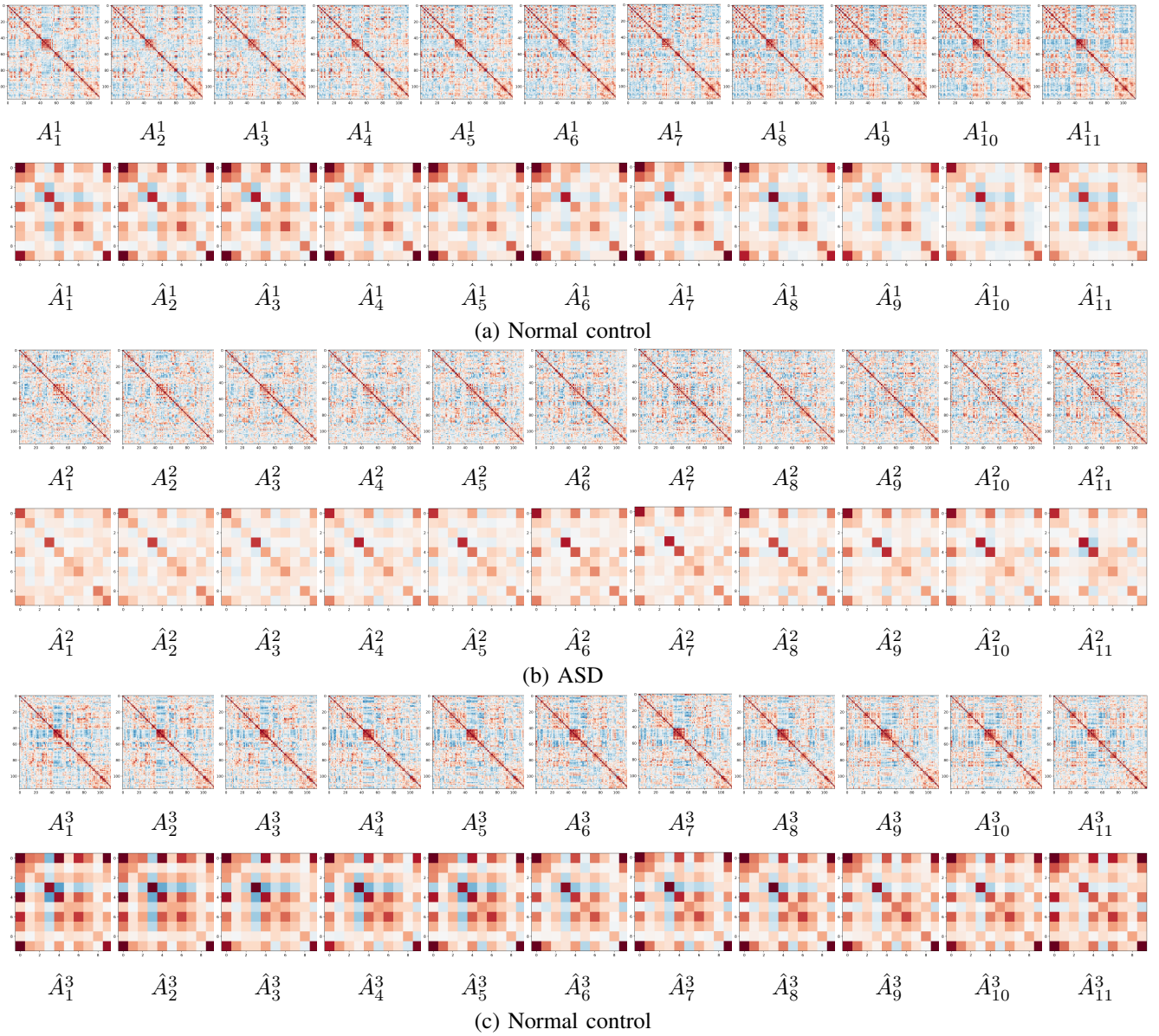


Fig. 7: Temporal multi-graph and temporal coarsened multi-graph of selected samples

where SN_e represents supernode e and SN_f represents supernode f . Following this definition, $score_p$ can also be interpreted as the sum of the product of the importance of any two nodes that belong to the sub-network p but within the same cluster.

Moreover, related studies have proved that inter-network connections in this system also play essential roles. To furtherly explore the critical cross-subnetwork correlation, the correlation score of two sub-networks S_p and S_q is calculated as:

$$score_{p,q} = \sum_{i \in S_p, j \in S_q \wedge i \in SN_e \wedge j \in SN_f \wedge e \neq f} F_{i,e} * F_{j,f} \quad (13)$$

where $score_{p,q}$ can also be interpreted as the sum of the product of the importance of any two nodes that belong to the sub-network p and sub-network q , respectively.

In this experiment, we evaluate six popular networks

including DMN(default mode network), CEN(central executive network), SN(salience network), AN(auditory network), SMN(somato-motor network), VN(visual network) using above formula. Through the weight calculated by (12) and (13), the top subnetworks and inter-subnetworks selected by our model are selected in Table IV. Moreover, we show these identified subnetworks in Fig. 8 and Fig. 9.

From Table IV, we find that the top four sub-networks are CEN, SN, SEN, DMN, which is consistent with the previous neuroscience studies [33], [34]. Neuroimaging studies have demonstrated that ASD is associated with the altered functional connectivity of CEN, DMN, and SN that are hypothesized to be central to the symptomatology of ASD.

In addition to the analysis of intra-subnetworks, we also analyze the interaction between sub-networks. We calculate that the top six sub-network connection strengths are (CEN, SMN), (CEN, SN), (CEN, AN), (DMN, SMN), (CEN, VN), (DMN,

TABLE IV: The rank of the intra-subnetworks as well as the top 6 cross inter-subnetworks selected and the corresponding weights optimized by our model

Intra-subnetworks		Correlation between subnetworks	
name	weight	name	weight
CEN	0.0186	(CEN, SMN)	0.0735
SN	0.0137	(CEN, SN)	0.0619
SEN	0.0121	(CEN, AN)	0.0602
DMN	0.0114	(DMN, SMN)	0.0593
VN	0.0100	(CEN, VN)	0.0587
AN	0.0092	(DMN, CEN)	0.0576

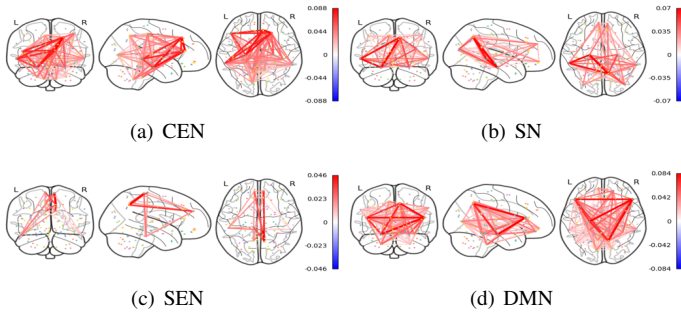


Fig. 8: The top 4 subnetworks identified by our BrainTGL.

CEN). The result is also consistent with prior knowledge regarding ASD. Neuroimaging research shows that ASD has a great relationship with the dysfunction of the triple network including CEN, SN, and DMN [35]. It is worth noting that SN, CEN, and DMN are often activated or deactivated together in attention-demanding tasks, which indicates that the network works synergistically to support attention and cognition. In addition, from a clinical point of view, the effect of a weak connection between DMN and SMN regions on ASD has been reported in the relevant literature. It is also consistent with our findings.

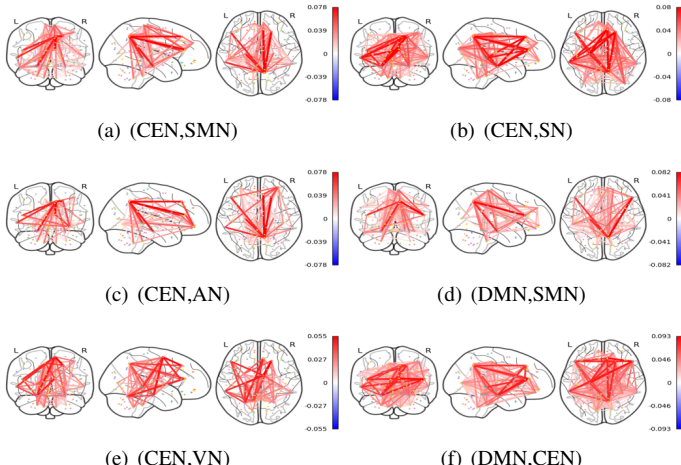


Fig. 9: The top 6 inter-subnetworks identified by our BrainTGL.

V. CONCLUSION

Recently, functional connectivity networks constructed from the functional magnetic resonance image (fMRI) hold great promise for understanding the functional mechanisms of human and brain distinguishing the patients with neurological disorders from Normal controls. Learning Dynamic Graph Embeddings is aimed at modeling spatio-temporal dynamics in Functional Brain Networks for improved classification performance. In order to achieve a better dynamic graph embedding from brain networks, we develop a temporal graph representation learning for Brain network (BrainTGL), which sufficiently exploit the spatio-temporal features in rs-fMRI data through temporal multi-graph clustering for removing noisy edge and dual temporal graph learning LSTM for learning temporal characteristics in fMRI data from two aspects. We conduct extensive experiments on real-world information networks to verify the effectiveness of our model, which demonstrates its superior performance compared with state-of-the-art baselines.

ACKNOWLEDGMENT

This research was supported by the National Natural Science Foundation of China (No.62076059) and the Fundamental Research Funds for the Central Universities (No. N2016001).

REFERENCES

- [1] D. Veitch, M. Weiner, P. Aisen, L. Beckett, N. Cairns, R. Green, D. Harvey, C. Jack, W. Jagust, J. C. Morris, R. Petersen, A. Saykin, L. Shaw, A. Toga, and J. Trojanowski, “Understanding disease progression and improving alzheimer’s disease clinical trials: Recent highlights from the alzheimer’s disease neuroimaging initiative,” *Alzheimer’s & Dementia*, vol. 15, pp. 106–152, 2019.
- [2] E. A. DeYoe, P. Bandettini, J. Neitz, D. Miller, and P. Winans, “Functional magnetic resonance imaging (fmri) of the human brain,” *Journal of neuroscience methods*, vol. 54, no. 2, pp. 171–187, 1994.
- [3] T. Safavi, C. Sripada, and D. Koutra, “Scalable hashing-based network discovery,” in *2017 IEEE International Conference on Data Mining (ICDM)*. IEEE, 2017, pp. 405–414.
- [4] B. Jie, M. Liu, D. Zhang, and D. Shen, “Sub-network kernels for measuring similarity of brain connectivity networks in disease diagnosis,” *IEEE Transactions on Image Processing*, vol. 27, no. 5, pp. 2340–2353, 2018.
- [5] B. Jie, D. Zhang, C.-Y. Wee, and D. Shen, “Topological graph kernel on multiple thresholded functional connectivity networks for mild cognitive impairment classification,” *Human brain mapping*, vol. 35, no. 7, pp. 2876–2897, 2014.
- [6] D. Yao, M. Liu, M. Wang, C. Lian, J. Wei, L. Sun, J. Sui, and D. Shen, “Triplet graph convolutional network for multi-scale analysis of functional connectivity using functional mri,” in *International Workshop on Graph Learning in Medical Imaging*. Springer, 2019, pp. 70–78.
- [7] T. Eslami, V. Mirjalili, A. Fong, A. R. Laird, and F. Saeed, “Asd-diagnt: a hybrid learning approach for detection of autism spectrum disorder using fmri data,” *Frontiers in neuroinformatics*, vol. 13, p. 70, 2019.
- [8] Y. Yan, J. Zhu, M. Duda, E. Solarz, C. Sripada, and D. Koutra, “Groupinn: Grouping-based interpretable neural network for classification of limited, noisy brain data,” in *Proceedings of the 25th ACM SIGKDD International Conference on Knowledge Discovery & Data Mining*, 2019, pp. 772–782.
- [9] S. Parisot, S. I. Ktena, E. Ferrante, M. Lee, R. G. Moreno, B. Glocker, and D. Rueckert, “Spectral graph convolutions for population-based disease prediction,” in *International conference on medical image computing and computer-assisted intervention*. Springer, 2017, pp. 177–185.
- [10] S. I. Ktena, S. Parisot, E. Ferrante, M. Rajchl, M. Lee, B. Glocker, and D. Rueckert, “Metric learning with spectral graph convolutions on brain connectivity networks,” *NeuroImage*, vol. 169, pp. 431–442, 2018.

- [11] R. M. Hutchison, T. Womelsdorf, E. A. Allen, P. A. Bandettini, V. D. Calhoun, M. Corbetta, S. Della Penna, J. H. Duyn, G. H. Glover, J. Gonzalez-Castillo *et al.*, "Dynamic functional connectivity: promise, issues, and interpretations," *Neuroimage*, vol. 80, pp. 360–378, 2013.
- [12] M. Wang, C. Lian, D. Yao, D. Zhang, M. Liu, and D. Shen, "Spatial-temporal dependency modeling and network hub detection for functional mri analysis via convolutional-recurrent network," *IEEE Transactions on Biomedical Engineering*, vol. 67, no. 8, pp. 2241–2252, 2019.
- [13] S. Gadgil, Q. Zhao, A. Pfefferbaum, E. V. Sullivan, E. Adeli, and K. M. Pohl, "Spatio-temporal graph convolution for resting-state fmri analysis," in *International Conference on Medical Image Computing and Computer-Assisted Intervention*. Springer, 2020, pp. 528–538.
- [14] T. Azevedo, A. Campbell, R. Romero-Garcia, L. Passamonti, R. A. Bethlehem, P. Lio, and N. Toschi, "A deep graph neural network architecture for modelling spatio-temporal dynamics in resting-state functional mri data," *bioRxiv*, 2020.
- [15] S. Vaishali, K. K. Rao, and G. V. S. Rao, "A review on noise reduction methods for brain mri images," *2015 International Conference on Signal Processing and Communication Engineering Systems*, pp. 363–365, 2015.
- [16] C. R. Pernet, R. R. Wilcox, and G. A. Rousselet, "Robust correlation analyses: false positive and power validation using a new open source matlab toolbox," *Frontiers in psychology*, vol. 3, p. 606, 2013.
- [17] D. C. Van Essen, S. M. Smith, D. M. Barch, T. E. Behrens, E. Yacoub, K. Ugurbil, W.-M. H. Consortium *et al.*, "The wu-minn human connectome project: an overview," *Neuroimage*, vol. 80, pp. 62–79, 2013.
- [18] A. Di Martino, C.-G. Yan, Q. Li, E. Denio, F. X. Castellanos, K. Alaerts, J. S. Anderson, M. Assaf, S. Y. Bookheimer, M. Dapretto *et al.*, "The autism brain imaging data exchange: towards a large-scale evaluation of the intrinsic brain architecture in autism," *Molecular psychiatry*, vol. 19, no. 6, pp. 659–667, 2014.
- [19] T. Kudo, E. Maeda, and Y. Matsumoto, "An application of boosting to graph classification," in *Advances in neural information processing systems*, 2004, pp. 729–736.
- [20] B. Cao, L. He, X. Wei, M. Xing, P. S. Yu, H. Klumpp, and A. D. Leow, "t-bne: Tensor-based brain network embedding," in *Proceedings of the 2017 SIAM International Conference on Data Mining*. SIAM, 2017, pp. 189–197.
- [21] R. P. Monti, P. Hellyer, D. Sharp, R. Leeched, C. Anagnostopoulos, and G. Montana, "Estimating time-varying brain connectivity networks from functional mri time series," *NeuroImage*, vol. 103, pp. 427–443, 2014.
- [22] B. Cai, G. Zhang, A. Zhang, J. M. Stephen, T. W. Wilson, V. D. Calhoun, and Y.-P. Wang, "Capturing dynamic connectivity from resting state fmri using time-varying graphical lasso," *IEEE Transactions on Biomedical Engineering*, vol. 66, no. 7, pp. 1852–1862, 2018.
- [23] C.-Y. Wee, S. Yang, P.-T. Yap, and D. Shen, "Sparse temporally dynamic resting-state functional connectivity networks for early mci identification," *Brain imaging and behavior*, vol. 10, no. 2, pp. 342–356, 2016.
- [24] B. Jie, M. Liu, and D. Shen, "Integration of temporal and spatial properties of dynamic connectivity networks for automatic diagnosis of brain disease," *Medical image analysis*, vol. 47, pp. 81–94, 2018.
- [25] M. Wang, J. Huang, M. Liu, and D. Zhang, "Modeling dynamic characteristics of brain functional connectivity networks using resting-state functional mri," *Medical image analysis*, vol. 71, p. 102063, 2021.
- [26] S. Yan, Y. Xiong, and D. Lin, "Spatial temporal graph convolutional networks for skeleton-based action recognition," in *Thirty-second AAAI conference on artificial intelligence*, 2018.
- [27] B. Yu, H. Yin, and Z. Zhu, "Spatio-temporal graph convolutional networks: A deep learning framework for traffic forecasting," *arXiv preprint arXiv:1709.04875*, 2017.
- [28] W. Tang, Z. Lu, and I. S. Dhillon, "Clustering with multiple graphs," in *2009 Ninth IEEE International Conference on Data Mining*. IEEE, 2009, pp. 1016–1021.
- [29] C. Cameron, S. Sharad, C. Brian, K. Ranjeet, G. Satrajit, Y. Chaogan, L. Qingyang, L. Daniel, V. Joshua, B. Randal, C. Stanley, M. Maarten, K. Clare, D. Adriana, C. Francisco, and M. Michael, "Towards automated analysis of connectomes: The configurable pipeline for the analysis of connectomes (c-pac)," *Frontiers in Neuroinformatics*, vol. 7, 2013.
- [30] M. Glasser, S. Sotiropoulos, J. A. Wilson, T. S. Coalson, B. Fischl, J. Andersson, J. Xu, S. Jbabdi, M. A. Webster, J. Polimeni, D. V. Essen, and M. Jenkinson, "The minimal preprocessing pipelines for the human connectome project," *NeuroImage*, vol. 80, pp. 105–124, 2013.
- [31] Y. Ma, S. Wang, C. C. Aggarwal, and J. Tang, "Graph convolutional networks with eigenpooling," in *Proceedings of the 25th ACM SIGKDD International Conference on Knowledge Discovery & Data Mining*, 2019, pp. 723–731.
- [32] P. W. Battaglia, J. B. Hamrick, V. Bapst, A. Sanchez-Gonzalez, V. Zamzaldi, M. Malinowski, A. Tacchetti, D. Raposo, A. Santoro, R. Faulkner *et al.*, "Relational inductive biases, deep learning, and graph networks," *arXiv preprint arXiv:1806.01261*, 2018.
- [33] A. Manoliu, V. Riedl, A. Zherdin, M. Mühlau, D. Schwerthöffer, M. Scherr, H. Peters, C. Zimmer, H. Förstl, J. Bäuml *et al.*, "Aberrant dependence of default mode/central executive network interactions on anterior insular salience network activity in schizophrenia," *Schizophrenia bulletin*, vol. 40, no. 2, pp. 428–437, 2014.
- [34] A. Manoliu, C. Meng, F. Brandl, A. Doll, M. Tahmasian, M. Scherr, D. Schwerthöffer, C. Zimmer, H. Förstl, J. Bäuml *et al.*, "Insular dysfunction within the salience network is associated with severity of symptoms and aberrant inter-network connectivity in major depressive disorder," *Frontiers in human neuroscience*, vol. 7, p. 930, 2014.
- [35] Y. Jiang, M. Duan, X. Chen, X. Chang, H. He, Y. Li, C. Luo, and D. Yao, "Common and distinct dysfunctional patterns contribute to triple network model in schizophrenia and depression: a preliminary study," *Progress in Neuro-Psychopharmacology and Biological Psychiatry*, vol. 79, pp. 302–310, 2017.